Oligomerization and aggregation of NAP-22 with several metal ions

Maekawa, Shohei
Yuzu, Keisuke
Chatani, Eri
Morigaki, Kenichi

Oligomerization and aggregation of NAP-22 with several metal ions

Shohei Maekawa*[1], Keisuke Yuzu[1], Eri Chatani[1], Kenichi Morigaki[2, 3]

1: Graduate School of Science, Kobe University, Rokkodaicho 1-1, Nada, Kobe 657-8501, Japan
2: Graduate School of Agricultural Science, Kobe University, Rokkodaicho 1-1, Nada, Kobe 657-8501, Japan
3: Biosignal Research Center, Kobe University, Rokkodaicho 1-1, Nada, Kobe 657-8501, Japan

*Corresponding author: Shohei Maekawa: E-mail: smaekawa@kobe-u.ac.jp

Abbreviations

IDP; intrinsically disordered protein, GA; glutaraldehyde, Native-PAGE; clear native polyacrylamide gel electrophoresis, XL-SDS-PAGE; SDS-PAGE after cross-linking with GA, Hepes10 buffer; 10 mM Hepes-KOH, 140 mM NaCl, pH 7.4, Hepes100 buffer; 100mM Hepes-KOH, 30 mM NaCl, pH 7.4, TPP; thiamine pyrophosphate, PLP; pyridoxal phosphate, PEA; phosphoryl ethanolamine, NAM; nicotinamide monoriboside, NAD^+; nicotinamide adenine dinucleotide, $NADP^+$; nicotinamide adenine dinucleotide phosphate, CoA; coenzyme A, TEM; transmission electron microscope.

Abstract

Metal ions participate in various biochemical processes such as electron transport chain, gene transcription, and enzymatic reactions. Furthermore, the aggregation promoting effect of several metal ions on neuronal proteins such as prion, tau, Aβ peptide, and α-synuclein, has been reported. NAP-22 (also called BASP1 or CAP-23) is a neuron-enriched calmodulin-binding protein and one of the major proteins in the detergent-resistant membrane microdomain fraction of the neuronal cell membrane. Previously, we showed oligomer formation of NAP-22 in the presence of several phospholipids and fatty acids. In this study, we found the aggregation of NAP-22 by $FeCl_2$, $FeCl_3$, and $AlCl_3$ using native-PAGE. Oligomer or aggregate formation of NAP-22 by $ZnCl_2$ or $CuSO_4$ was shown with SDS-PAGE after cross-linking with glutaraldehyde. Morphological analysis with electron microscopy revealed the formation of large aggregates composed of small annular oligomers in the presence of $FeCl_3$, $AlCl_3$, or

$CuSO_4$. In case of $FeCl_2$ or $ZnCl_2$, instead of large aggregates, scattered annular and globular oligomers were observed. Interestingly, metal ion induced aggregation of NAP-22 was inhibited by several coenzymes such as $NADP^+$, NADPH, or thiamine pyrophosphate. Since NAP-22 is highly expressed in the presynaptic region of the synapse, this result suggests the participation of metal ions not only on the protein and membrane dynamics at the presynaptic region, but also on the metabolic regulation though the interaction with coenzymes.

Key words: neuron, synapse, membrane, NAP-22 oligomerization, metal ions, protein aggregation, coenzymes

Introduction

NAP-22(also called CAP-23 or BASP1) is a major protein of mammalian brain localized predominantly in the presynaptic region of the neuron [9, 13-16, 21]. It is also one of the main proteins of the detergent-resistant membrane microdomain fraction of brain and hence is considered to reside in the raft domain [17,18]. Since knockout mice lacking NAP-22 exhibited a pronounced and complex phenotype, including a defect to produce stimulus-induced nerve sprouting at the adult neuromuscular junction, participation of NAP-22 in the regulation of the cytoplasmic structures and membrane dynamics at the synaptic region was considered [6]. In fact, further studies showed the interaction of NAP-22 with various proteins such as calmodulin [14], actin capping protein (CapZ)[22], synaptojanin-1[28], glutamate decarboxylase [19], and dynamin [30]. In addition, NAP-22 binds acidic lipids such as phosphatidylserine, phosphatidylglycerol, phosphatidylinositol, phosphatidylinositol phosphates, cardiolipin, and gangliosides [12, 20, 29]. NAP-22 is considered as an intrinsically disordered protein (IDP), for physicochemical characterization of NAP-22 showed that it is resistant to various hard treatment such as boiling (95℃, 5min) or acid (2.5% perchloric acid, 20 min on ice) and has poor higher order structure [29, 33]. Since IDP has been recognized to participate various cellular functions, further studies on the identification of another interaction partners of NAP-22 and characterization of the interaction could be a good clue to understand the molecular background of cells. In fact, participation of NAP-22 in the regulation of gene expression in the nucleus through the interaction with WT1(Wims' tumor suppressor protein) or estrogen receptor was recently reported [8]. Furthermore, the presence of a high-affinity cocaine binding site associated with NAP-22 was reported, although the precise mechanism of the binding has not been analyzed [7].

Self-association (oligomerization) of NAP-22 was first indicated through physicochemical analysis of solubilized NAP-22 [4]. Oligomerization of NAP-22 was further studied by Zakharov and Mosevitsky and they showed circular association of 10-14 monomers and formation of a tubular or cylindrical structure on the nitrocellulose membrane at low ionic condition. Interestingly, they showed that low concentration of SDS induces the oligomer of NAP-22 composed of 8~14 monomers [5, 33]. Previously, we showed the presence of a broad NAP-22 oligomer band at very large molecular mass region (500~600 kDa) in SDS-PAGE after cross-linking with glutaraldehyde (GA). And transmission electron microscope (TEM) observation showed annular or oval structures (~10 nm wide) of the oligomer. Since these annular or oval structures were also observed in huge NAP-22 complexes (aggregates) formed in the presence of several fatty acids and phospholipids, we judged the aggregates were formed through the assembly of the oligomers [23].

Oligomerization or aggregation of several proteins or peptides such as prion, tau, α-synuclein, and Aβ peptide has been paid much attention for these oligomers or aggregates are considered to have toxic effects on the neuronal functions [2, 11, 27, 31]. Since several metal ions have shown to promote the aggregate formation of these proteins, dysregulation of metal ion homeostasis is considered as one of the etiologies of the Alzheimer's disease, Parkinson' s disease, and prion disease [3, 11, 24, 25].

Considering the high expression of NAP-22 in the presynaptic region of the neuron, the effect of several metal ions on the oligomer/aggregate formation of NAP-22 was studied and found that $FeCl_2$, $FeCl_3$, $AlCl_3$ and $CuSO_4$ induced the aggregation of NAP-22. SDS-PAGE after cross-linking with glutaraldehyde showed the oligomerization effect of $ZnCl_2$. Interestingly, some coenzymes inhibited metal ion induced aggregation of NAP-22. This result suggests the possible participation of metal ions not only on the protein dynamics but also on the metabolic regulation of cells.

Materials and Methods

1. Proteins and chemical reagents

Myristoylated NAP-22 and non-myristoylated NAP-22 were expressed in bacteria and purified as described [16, 30]. Metal ions were obtained from Nacalai Tesc (Japan) and Wako-FujiFilm (Japan). Other chemicals were obtained from Oriental yeast(Japan)(NAD^+, NADH, $NADP^+$, NADPH, CoA), from Sigma-Aldrich(USA)(TPP; thiamine pyrophosphate), from Nakacai Tesc(Japan)(PLP; pyridoxal phosphate, PEA; phosphoryl ethanolamine), from Wako-FujiFilm(Japan)(pyridoxine, acetyl-CoA),

TCI(Japan)(pyridoxamine), and from Adooq BioScience(USA)(NAM; nicotine amide monoriboside).

2. Reaction and electrophoresis

Purified NAP-22(0.048 mg/ml) (2.2 μM) in Hepes100-buffer (100 mM Hepes-KOH, 30 mM NaCl, pH 7.4) was incubated at 37℃ for 20 min in the presence or absence of various metal ions. In some experiments, longer incubation time (60 min or 180 min) was attempted. Clear-Native-PAGE was done using 3.8% acrylamide gel for stacking and 4%～16% linear acrylamide gradient gel for separation according to Schagger et al. after the addition of 1/3 vol of 60% glycerol [26]. In case of XL-SDS-PAGE, cross-linking was done by addition of 1/9 vol of 0.6% glutaraldehyde (GA) solution after the first incubation. Samples were further incubated for 20 min at 37℃. GA was then blocked with the SDS-sample buffer. After boiling for 2 min, samples were analyzed with SDS-PAGE using 3.8% stacking gel and 11% acrylamide gel for separation. Precision protein markers (Bio-Rad) were used, and gel staining and de-staining was done as described previously [23].

3. Centrifugation assay

Incubated samples were centrifuged at 100,000 xg for 30 min at 4℃ and the supernatant fraction (sup) was recovered and boiled for 2 min after the addition of SDS-sample buffer. The pellet fraction (ppt) was suspended in the SDS-sample buffer containing 10 mM EDTA, sonicated (3x 30sec), incubated for 20 min at RT, and boiled before electrophoresis.

4. Electron microscopy

TEM images were obtained using a JEM-1010 transmission electron microscope (JEOL, Tokyo, Japan) with a voltage of 100 kV. Usually, NAP-22 (0.048 mg/ml (2.2 μM)) in Hepes10 buffer (10 mM Hepes-KOH, 0.14 M NaCl, pH 7.4) with or without metal ions was incubated for 20 min at 37℃. The sample was then diluted 3-fold with the Hepes10 buffer and mounted on a collodion-coated 400-mesh grid for 5 min at RT. After three times wash with distilled water, samples were negatively stained with 4x-diluted EM stainer (Nisshin EM, Tokyo, Japan) for 3 min [23, 32].

5. Statistical analysis

Data are presented as mean ± SD. In case of ellipsoidal structures, large axis/short axis were shown. Student's *t*-test was used for statistical comparisons and $P < 0.05$ was considered statistically significant.

Results

1. Native-PAGE and XL-SDS-PAGE analysis of the effect of metal ions.

Since the formation of high molecular mass complex of NAP-22 in the presence of some acidic phospholipids and gangliosides was shown with Clear Native-Page (Native-PAGE) in previous studies [12, 23], the effect of metal ions on the formation of high molecular mass complex of NAP-22 was firstly studied with Native-PAGE. Fig. 1A(left) shows that the presence of $MgCl_2$, $CaCl_2$, $ZnCl_2$, $CuSO_4$, or $MnCl_2$, caused little or no mobility change of NAP-22 in Native-PAGE. On the other hand, in the presence of two iron ions, $FeCl_2$ and $FeCl_3$, and $AlCl_3$, the monomeric band of NAP-22(black arrow) was not detected in the lane, suggesting the formation of very large aggregates that cannot enter the 3.8% acrylamide gel. In case of $FeCl_2$, the presence of high molecular mass smearing band in the gel (arrowhead) and protein complexes that were trapped at the top of 3.8% gel (white arrow) were detected.

Next, in order to detect oligomer formation with metal ions, SDS-PAGE analysis after cross-linking with glutaraldehyde (GA) (XL-SDS-PAGE) was attempted (Fig. 1A right). In the absence of metal ions, NAP-22 moved mainly as the monomer (black arrow) and a very faint smear band was detected in the high molecular region. In the presence of Mg^{2+}, Ca^{2+} or Mn^{2+}, in addition to the monomer band, a faint band of NAP-22 was detected in the high molecular weight region. Interestingly, in the presence of Zn^{2+}, a clear broad band of NAP-22 was detected in the same region(arrowhead) and the protein staining at the monomer region decreased. Since NAP-22 oligomer composed of 8~12 monomers was reported to be electrophoresed in this high molecular mass region in the previous report [23], this result suggests the formation of oligomer by Zn^{2+} ions. In the presence of Fe ions (Fe^{2+}, Fe^{3+}) and Al^{3+}, NAP-22 was poorly detected in the gel, suggesting the formation of very large aggregates. A part of the aggregate was detected in the Fe^{2+} lane at the top of the gel (white arrow). In case of Cu^{2+}, in contrast to the result of Native-PAGE, SDS-PAGE after cross-linking (XL-SDS-PAGE) showed no protein band at the monomer nor the oligomer region, suggesting large aggregate formation in the presence of Cu^{2+} ion. Monomer detection in Zn^{2+} and Cu^{2+} lanes in Native-PAGE suggests that the interaction of these two ions to NAP-22 is not strong enough to keep a complex during Native-PAGE (under Native-PAGE, metal ions moved to the cathode, and NAP-22, an acidic protein, moves to the anode). Using non-

myristoylated NAP-22, the same experiments were done (Fig. 1B). Since basically same results were obtained, the myristoyl-moiety was judged not to contribute to the metal ion induced aggregation or oligomerization.

Next, the effective metal ion concentration for the NAP-22 aggregation was studied. In Native-PAGE, $FeCl_2$, $FeCl_3$, and $AlCl_3$ showed some effect at 0.5 mM and the monomer band was almost disappeared at 1 mM (Supplementary file, Fig. S1). Since the effects of Zn^{2+} and Cu^{2+} ions were detected with the XL-SDS-PAGE method, this method was used to detect the effect of Fe, Zn, and Cu ions on NAP-22 at more low concentration and longer incubation time. Significant decrease of NAP-22 monomer at 0.2 mM concentration after 60 min incubation was detected (Fig. 2). In case of $FeCl_2$ or $ZnCl_2$, the oligomer/aggregation formation activity was evident at 10 μM concentration. In case of $FeCl_3$ and $CuSO_4$, 20 μM concentration was need to detect the aggregate formation. Further attempt of oligomer formation at 5 μM concentration for 180 min incubation showed no significant effect (data not shown).

2. Analysis of the aggregate formation with centrifugation

Since centrifugation is an effective method to detect protein polymerization or aggregation, the incubated samples were centrifuged at 100,000 xg for 30min at 4℃, and the supernatant and the pellet fractions were analyzed with SDS-PAGE (Fig. 3). In the absence of metal ions, large part of the protein was recovered in the supernatant fraction. In the presence of $FeCl_2$, $FeCl_3$, and $AlCl_3$, the amount of NAP-22 in the supernatant was decreased and the protein amount in the pellet fraction was increased in a dose-dependent manner. On the other hand, the addition of $ZnCl_2$, $MnCl_2$, $MgCl_2$, or $CaCl_2$, caused no increase of the amount of the protein in the pellet fractions. In case of $CuSO_4$, some increase of the protein in the pellet fraction was observed at 2 mM concentration (Fig. 3). Poor sedimentation of $ZnCl_2$-induced oligomers in the centrifugation and the detection of a broad cross-linked oligomer band in the XL-SDS-PAGE (Fig. 1A) suggested that the $ZnCl_2$-induced oligomer was smaller than the aggregate formed in the presence of $FeCl_2$, $FeCl_3$, or $AlCl_3$(vide infra).

3. Morphology of the oligomers

The structure of the oligomers/aggregates was then observed with an electron microscope after negative staining (Fig. 4. Upper; low magnification, lower; high magnification, Supplementary file: Fig. S2). In the presence of $FeCl_2$, widely scattered globular structures were observed. At high magnification, in addition to the globular structures, many annular structures were also observed (showed with arrows). The

annular structures were looked like elliptical rather than circular and measurement of the lengths confirmed this result (long axis; 26.2±3.21nm, short axis; 21.2±2.45nm) (Table in SF (supplementary file)). In case of $FeCl_3$, very large amorphous aggregates composed of filamentous structures were observed at low magnification. At high magnification, many annular structures looked like packaged in the aggregates were observed, and the size of the annular structures was much smaller than that observed in $FeCl_2$ solution (long axis; 13.3±1.50 nm, short axis; 11.42±1.44 nm). In case of $CuSO_4$, very large globular aggregates were observed in low magnification, but the number of the large aggregates was very few compared to that observed in case of $FeCl_3$. Many small oval structures were observed in the aggregates at high magnification. Their size (long axis; 8.33 ±1.45 nm, short axis; 6.77 ±1.16 nm) was much smaller than that observed in $FeCl_3$ solution. Since many scattered oligomers were observed at high magnification, large part of NAP-22 was assumed to be oligomeric form in $CuSO_4$ solution. In case of $ZnCl_2$, large amorphous aggregates were hardly detected. Instead, short small circular structures widely scattered on the mesh were observed at low magnification. At high magnification, both annular structures(arrows) and ellipsoidal structures with no hole were observed. The ellipsoidal structures could be the side-face of the annular structures. Higher magnified figures of $ZnCl_2$-, and $CuSO_4$-treated samples are shown in SF (Fig. S3). In case of $AlCl_3$, aggregated oligomers similar to the case of $FeCl_3$ were observed. The size of the annular structures in the aggregates were much larger than that of $FeCl_3$(long axis; 19.51 ± 1.76 nm, short axis; 17.40 ± 1.43 nm) (SF: Fig. S2).

4. Inhibitory effect of several coenzymes on the metal ion induced aggregation of NAP-22

Considering the membrane localization of NAP-22 in neurons and nuclear localization in several cells, metal ions could participate in the membrane dynamics and/or gene expression through the oligomerization/aggregation of NAP-22. In order to know the possible regulatory mechanisms of NAP-22 aggregation, the effect of several biomolecules on the NAP-22 aggregation by metal ions was screened using Native-PAGE (Fig. 5). Among tested compounds, TPP (thiamine pyrophosphate) (lane 11) showed inhibitory effect on $FeCl_2$ or $FeCl_3$ induced aggregation. $NADP^+$(lane 4), NADPH (lane 6), CoA (lane 13), and acetyl-CoA (lane 14) also showed inhibitory effect on $FeCl_2$ induced aggregation and showed lesser effect on $FeCl_3$ induced aggregation. PLP (pyridoxal phosphate) (lane 7) reduced the size of the $FeCl_2$ induced

oligomers. Interestingly, NAD^+(lane 3) or NADH (lane 5) showed little effect on the aggregation of NAP-22 by $FeCl_2$ or $FeCl_3$.

Discussion

In this study, we reported that several metal ions induce the oligomerization or aggregate formation of NAP-22, a highly expressed protein in the presynaptic region of neurons. The aggregate formation by $FeCl_2$, $FeCl_3$, and $AlCl_3$ was confirmed with Native-PAGE, and the formation of oligomer by $ZnCl_2$ and the formation of aggregates by $CuSO_4$ were shown with SDS-PAGE after cross-linking using glutaraldehyde. The centrifugation assay confirmed these results.

Several metal ions have been shown to promote the aggregate formation of neuronal proteins such as prion, tau, α-synuclein, and Aβ peptide and the deposition of these metal ions on the amyloid plaques, Levy- bodies, tangles of tau and prion proteins [1-3, 11, 27]. Dysregulation of metal ion homeostasis is hence considered as one of the etiologies of the Alzheimer's disease, Parkinson's disease, and prion disease [2, 3, 11, 24, 25, 31]. To follow the amyloid formation, fluorescence change of thioflavin T is commonly used. For example, α-synuclein (35μM) was incubated with each 2 mM of $AlCl_3$, or $FeCl_3$, or $ZnCl_2$ for over 40 hr at 37°C, or Aβ peptide (4.8μM) was incubated with 1 mM $ZnCl_2$ or 0.25 mM $AlCl_3$ for 24 hr at 37°C (2, 3, 11, 25). Since the effective concentration of these metals on NAP-22 oligomerization/aggregation was 10 μM ($FeCl_2$ and $ZnCl_2$) and 20 μM ($CuSO_4$ and $FeCl_3$) (Fig.2) for 60 min incubation of 2.2μM NAP-22, self-association of NAP-22 is judged to occur under mild conditions compared to these amyloid proteins. The combination of Native-PAGE, XL-SDS-PAGE, and ultracentrifugation could be a good tool to identify new metal-dependent oligomer forming proteins.

Brain is a very complicated tissue composed of various types of neurons, glial cells, blood vessels, and so on. And metal ions interact with various proteins and small metabolites within cells. No precise data on the free concentration of these metal ions at the presynaptic region of neurons are available now. At present, hence, we have no data on the interaction of NAP-22 with metal ions in physiological or pathological conditions within neurons. Considering the highly localized presence of metal ions detected in the brain section analysis [1-3, 11] and the high expression of NAP-22 in the presynaptic region [9], oligomerization or aggregation of NAP-22 by these metal ions within neurons could be possible. Considering the poor effect of the myristoyl-moiety on the metal-ion induced oligomerization/aggregation, these metal ions could affect the membrane dynamics of neurons through the oligomerization/aggregation of membrane

bound NAP-22. Immunological studies on the oligomerization/aggregation of NAP-22 within cultured neurons supplemented with these metal ions are under investigation. Further studies on the histochemical analysis of the NAP-22 aggregates in the brains of Alzheimer-type transgenic mice or human brain could be very interesting.

Electron microscopic analysis also showed the formation of large NAP-22 aggregates in the presence of $FeCl_3$, $CuSO_4$ (Fig. 4), or $AlCl_3$ (SF, Fig. S2). In the presence of $FeCl_2$ or $ZnCl_2$, instead of large aggregates, scattered small annular oligomers were observed (Fig. 4). Considering that, in Native-PAGE, almost all NAP-22 moved as the monomer in the presence of $ZnCl_2$, or $CuSO_4$, small annular oligomers observed in the presence of these metal ions could be dissociated during Native-PAGE. In the presence of $FeCl_2$, NAP-22 detected at the top and at a broad range in the Native-PAGE gel (Fig. 1A). This could be the result of slow dissociation of NAP-22 from the oligomer during electrophoresis. In XL-SDS-PAGE, $ZnCl_2$- treaded sample showed a broad band at a high molecular mass region. This band could correspond to the scattered oligomers observed in Fig. 4 and Fig. S3.

In a previous study, the formation of tangled rope-like structures composed of oval or annular shaped oligomers in the presence of some phospholipids and fatty acids was reported [23]. In this study, the tangled rope-like structures were not observed. The size of small annular oligomers observed in samples of $ZnCl_2$-treated or $CuSO_4$-treated samples was nearly same with the size of oligomers observed phosphatidylserine-treated NAP-22 [23]. On the other hand, the size of $FeCl_2$-induced oligomers is much larger, and that of $FeCl_3$-induced oligomer is slightly larger than that of $ZnCl_2$-treated or $CuSO_4$-treated samples. In the previous study, protein samples were cross-linked with GA to preserve the structure during the SDS treatment used to remove phospholipids or fatty acids. The protein structures observed here were not cross-linked, direct comparison of the size of the structures is hence not appropriate. Since the small annular structure was observed in the large aggregates, this structure seems to be the basic oligomer of NAP-22 and further aggregation of the basic oligomer could result in the formation of large aggregates. In case of $ZnCl_2$, the latter aggregation process seems not likely to occur.

The molecular mechanism of metal ion-induced NAP-22 oligomerization is unclear at present. Since metal ions used here are bivalent or trivalent cations, cross-bridge of side-chains of acidic amino acid residues through ionic interaction could be a possible mechanism to induce oligomer formation. Stronger ionic interaction of trivalent cations may help to develop cross-bridge between proteins. Formation of large aggregates in the

presence of trivalent cations ($Fe^{3+}$and Al^{3+}) supports this idea. The difference in oligomer size may reflect the difference of amino acid residues used to cross-bridge.

Interestingly, some coenzymes inhibited metal ion induced oligomerization of NAP-22. The direct binding of these coenzymes to the metal ions or to the protein could be the inhibitory mechanism. In fact, direct binding of TPP with Cu^{2+}or Zn^{2+} has been reported [10]. Although further investigations are needed to elucidate the inhibitory mechanism, interaction of metal ions with intracellular small biomolecules such as coenzymes could be an important viewpoint to understand the function of metal ions within cells.

Acknowledgement
We thank Dr. Fumio Hayashi (Graduate School of Science, Kobe-University) for valuable discussions during experiments and preparation of the manuscript.

Authors statement
Shohei Maekawa and Kenichi Morigaki designed and performed the experiments, collected the data, and wrote the paper. TEM observation of NAP-22 oligomers/aggregates and critical discussions of the data were performed by Keisuke Yuzu and Eri Chatani.

Funding The research did not receive any specific grant from funding agencies in the public, commercial, or not-for profit sectors.

Declarations of Competing Interest
The authors declare that they have no conflict of interest.

References
[1]. Becker JS, Matusch A, Palm C, Salber D, Morton KA, Becker JS. Bioimaging of metals in brain tissue by laser ablation inductively coupled plasma mass spectrometry (LA-ICP-MS) and metallomics. Metallomics 2: 104-111(2010).

[2]. Chen L-L, Fan Y-G, Zhao L-X, Zhang Q, Wang Z-Y. The metal ion hypothesis of Alzheimer's disease and the anti-neuroinflammatory effect of metal chelators. Bioinorg. Chem. 131 (2013) 106301.

[3]. Das N, Raymick J, Sarkar S. Role of metals in Alzheimer's disease. Metabolic Brain Disease. 36:1627-1639 (2021).

[4]. Epand RM, Braswell EH, Yip CM, Epand RF, Maekawa S. Quaternary structure of the neuronal protein NAP-22 in aqueous solution. Biochim. Biophys. Acta 1650: 50-58 (2003).

[5]. Forsova OS, Zakkarov VV. High-order oligomers of intrinsically disorder brain proteins BASP1 and GAP-43 preserve the structural disorder. FEBS J. 283: 1550-1569 (2016).

[6]. Frey D, Laux T, Schneider C, Caroni P. Shared and unique roles of CAP23 and GAP43 in actin regulation, neurite outgrows, and anatomical plasticity. J Cell Biol. 149: 1443-54 (2000).

[7]. Harraz MM, Malla AP, Sermenza ER, Shishikura M, Singh M, Hwang Y, Kang IG, Song YJ, Snowman AM, Cortes P, Karuppagounder SS, Dawson TM, Dawson VL, Snyder SH. A high-affinity cocaine binding site associated with the brain acid soluble protein 1. Proc. Natl. Acad. Sci. USA 119 No.16 e2200545119 (2022).

[8]. Hartl M, Schneider RW. Unique family of neuronal signaling proteins implicated in oncogenesis and tumor suppression. Front. Oncol. 9: 289 (2019).

[9]. Iino S, Kobayashi S, Maekawa S. Immunohistochemical localization of a novel acidic calmodulin-binding protein NAP-22, in the rat brain. Neuroscience 91: 1435-1444 (1999).

[10]. Katz HB, Kustin K. Thiamine pyrophosphate-metal ion complexation: equilibrium and kinetics. Biochim. Biophys. Acta. 313: 235-248 (1973).

[11]. Kawahara M, Kato-Negishi M, Tanaka K. Amyloids: Regulation of metal homeostasis in the synapse. Molecules 25: 1441; doi:10.3390/molecules25061441, (2020)

[12]. Kobayashi Y, da Silva R, Kumanogoh H, Miyata S, Sato C, Kitajima K, Nakamura S, Morita M, Hayashi F, Maekawa S. Ganglioside contained in the neuronal

tissue-enriched protein of 22 kDa (NAP-22) fraction prepared from the detergent-resistant membrane microdomain of rat brain inhibits the phosphatase activity of calcineurin. J. Neurosci. Res. 93: 1462-1470 (2015).

[13]. Laux T, Fukami K, Thelen M, Golub T, Frey D, Caroni P. GAP43, MARCKS, and CAP23 modulate PI (4,5) P2 at plasmalemmal rafts, and regulate cell cortex actin dynamics through a common mechanism. J. Cell Biol. 149: 1455-1471(2000).

[14]. Maekawa S, Maekawa M, Hattori S, Nakamura S. Purification and molecular cloning of a novel acidic calmodulin binding protein from rat brain. J. Biol. Chem. 268: 13703-13709 (1993).

[15]. Maekawa S, Murofushi H, Nakamura S. Inhibitory effect of calmodulin on phosphorylation of NAP-22 with protein kinase C. J. Biol. Chem. 269: 19462-19465 (1994).

[16]. Maekawa S, Matsuura Y, Nakamura S. Expression and myristoylation of NAP-22 using a baculovirus transfer vector system. Biochim. Biophys. Acta 1218: 119-122 (1994).

[17]. Maekawa S, Kumanogoh H, Funatsu N, Takei N, Inoue K, Endo Y, Hamada K, Sokawa Y. Identification of NAP-22 and GAP-43(neuromodulin) as major protein components in a Triton insoluble low density fraction of rat brain. Biochim. Biophys. Acta 1323**:** 1-5 (1997)

[18]. Maekawa S, Sato C, Kitajima K, Funatsu N, Kumanogoh H. Sokawa Y. Cholesterol dependent localization of NAP-22 on a neuronal membrane microdomain (raft). J. Biol. Chem. 274: 21369-21374 (1999).

[19]. Maekawa S, Kobayashi Y, Odagaki, S-I, Makino M, Kumanogoh H, Nakamura S, Morita M, Hayashi F. Interaction of NAP-22 with brain glutamic acid decarboxylase(GAD). Neurosci. Lett. 537: 50-54 (2013).

[20]. Maekawa S, Kobayashi Y, Morita M, Suzaki T. Tight binding of NAP-22 with acidic membrane lipids. Neurosci. Lett. 600: 244-248 (2015).

[21]. Mosevitsky MI. Nerve ending “signal” proteins GAP-43, MARCKS and BASP1. Int. Rev. Cytol. 245: 245-325 (2005).

[22]. Odagaki S-I, Kumanogoh H, Nakamura S, Maekawa S. Biochemical interaction of an actin capping protein, CapZ, with NAP-22. J. Neurosci. Res. 87: 1980-1985 (2009).

[23]. Odagaki S-I, Maekawa S, Hayashi F, Suzaki T, Morigaki K. The effect of phospholipids and fatty acids on the oligomer formation of NAP-22. Neurosci. Lett. 736: 135288 (2020).

[24]. Peng YX, Chang X, Lang M. Iron homeostasis disorder and Alzheimer’s disease. Int. J. Mol. Sci. 22, 12442 (2021).

[25]. Quintanar L, Lim MH. Metal ions and degenerative diseases. J. Biol. Inorg. Chem. 24: 1137-1139 (2019).

[26]. Schagger H, Cramer WA, von Jagow G. Analysis of molecular masses and oligomeric states of protein complexes by blue native electrophoresis and isolation of membrane protein complexes by two-dimensional native electrophoresis, Anal. Biochem. 217: 261-270 (1994).

[27]. Sigurdson CJ, Bartz JC, Glatzel M. Cellular and molecular mechanisms of prion disease. Annu. Rev. Pathol. 14: 497-516 (2019)

[28]. Takaichi R, Odagaki S-I, Kumanogoh H, Nakamura S, Morita M, Maekawa S. Inhibitory effect of NAP-22 on the phosphatase activity of synaptojanin-1. J. Neurosci. Res. 90: 21-27 (2012).

[29]. Terashita A, Funatsu N, Umeda M, Shimada Y, Ohno-Iwashita Y, Epand RM, Maekawa S. Lipid binding activity of a neuron-specific protein NAP-22 studied in vivo and in vitro. J. Neurosci. Res. 70: 172-179 (2002).

[30]. Ueno S, Miyoshi H, Maruyama Y, Morita M, Maekawa S. Interaction of dynamin I with NAP-22, a neuronal protein enriched in the presynaptic region. Neurosci. Lett. 675: 59-63 (2018).

[31]. Wong YC, Krainc D. α-synuclein toxicity in neurodegeneration: mechanism and therapeutic strategies. Nat. Med. 23:1-13 (2017)

[32]. Yuzu K, Yamamoto N, Noji M, So M, Goto Y, Iwasaki T, Tsubaki M, Chatani E. Multistep changes in amyloid structure induced by cross-seeding on a rugged energy landscape. Biophys. J. 120: 284-295 (2021).

[33]. Zakharov VV, Mosevitsky MI. Oligomeric structure of brain abundant proteins GAP-43 and BASP1. J. Struct. Biol. 170: 470-483(2010).

Figure legends

Figure 1. Effect of metal ions on the oligomerization/aggregation of NAP-22. The effect metal ions on myristoylated NAP-22 (A) and non-myristoylated NAP-22 (B) was studied using Native-PAGE or SDS-PAGE after cross-linking with glutaraldehyde (XL-SDS-PAGE). Samples were incubated with/without 2 mM ion for 20 min at 37℃ and electrophoresed. Lane represents, –; no metal, Mg; $MgCl_2$, Ca; $CaCl_2$, Fe; $FeCl_2$, Fe^{3+}; $FeCl_3$, Cu; $CuSO_4$, Mn; $MnCl_2$, Al^{3+}; $AlCl_3$. The bands of monomer are shown by black arrows and the bands of slow-moving component are shown by arrowheads. The bands at the top of the gels are shown by white arrows. The positions of molecular markers are shown at the right side of the XL-SDS-PAGE gel (B).

Figure 2. Dose-dependent effect of metal ions on the oligomerization/aggregation of NAP-22 studied with XL-SDS-PAGE after the incubation at 37℃ for 60 min.
After XL-SDS-PAGE, protein amount in the monomer region of the gel was measured using imageJ and represented as % to the amount without the metal ion. Average values are shown with SD(N=4). The lowest significant concentration (**) (p-value) was, $FeCl_2$; 10μM (0.0016), $FeCl_3$; 20μM (0.003), $ZnCl_2$; 10μM (0.0004), $CuSO_4$; 20μM (0.0025).

Figure 3. Centrifugation assay of the oligomerization of NAP-22. After incubation for 20 min at indicated ion concentration, samples were centrifuged at 100,000 xg for 30min (4℃). Whole amount of the supernatant fraction (sup) and pellet fraction (ppt) was analyzed with SDS-PAGE. In lane “w”, whole amount of protein used in the analysis was applied. Only the appropriate region of the gel is shown.

Figure 4. Negative stained NAP-22 oligomers/aggggregates observed after incubation with indicated metal ions (2 mM) were shown in low (upper) and high magnification (lower). Annular structures were indicated with white arrows in the lower panel.

Figure 5. Inhibitory effect of several coenzymes on the NAP-22 oligomerization by $FeCl_2$ or $FeCl_3$. In lane 1, NAP-22 was incubated without metal ion. In lane 2~14, NAP-22 was incubated with 2 mM $FeCl_2$(A) or $FeCl_3$(B)(lane 2) and each 2 mM of NAD^+ (nicotine amide adenine dinucleotide), (lane 3), $NADP^+$ (nicotine amide adenine dinucleotide monophosphate), (lane 4), NADH (lane 5), NADPH (lane 6), PLP(pyridoxal phosphate) (lane 7), phosphoryl ethanolamine (lane 8), pyridoxine (lane 9), pyridoxamine (lane 10), TPP (thiamine pyrophosphate)(lane 11), NAM(nicotine amido monoriboside) (lane 12), CoA (lane 13), and acetyl-CoA (lane 14).

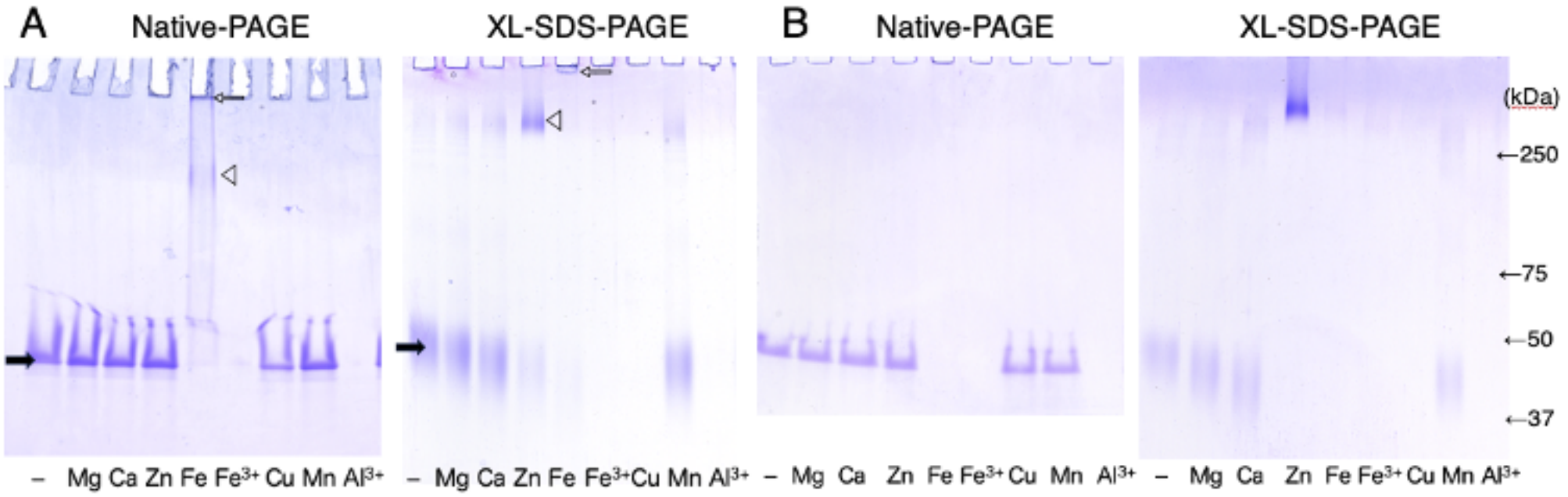
A
Native-PAGE
XL-SDS-PAGE
B
Native-PAGE
XL-SDS-PAGE
(kDa)
←250
←75
←50
←37
– Mg Ca Zn Fe Fe3+ Cu Mn Al3+
– Mg Ca Zn Fe Fe3+ Cu Mn Al3+
– Mg Ca Zn Fe Fe3+ Cu Mn Al3+
– Mg Ca Zn Fe Fe3+ Cu Mn Al3+

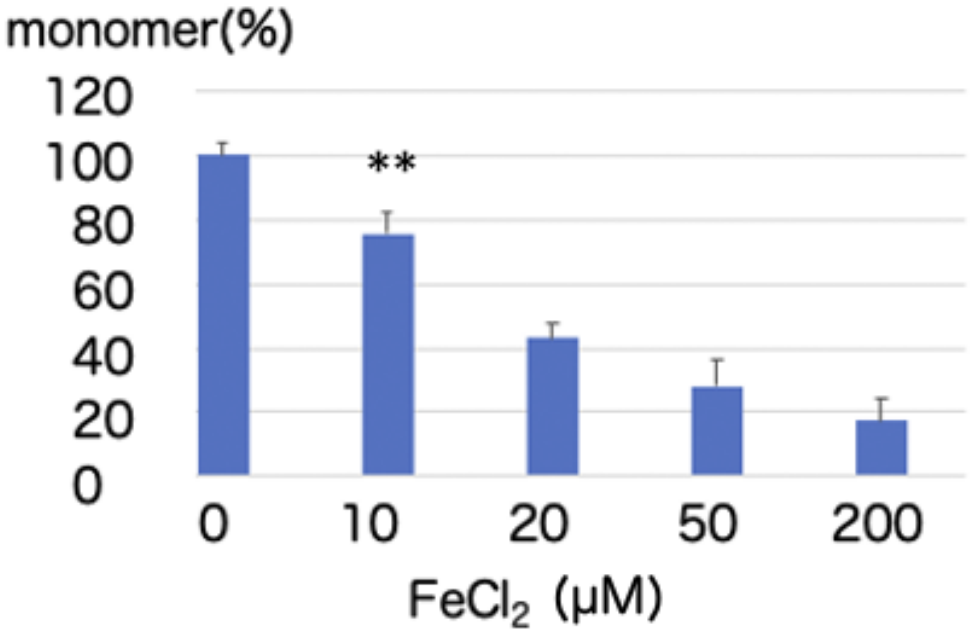
monomer(%)
120
100
80
60
40
20
0
**
0
10
20
50
200
FeCl2 (μM)

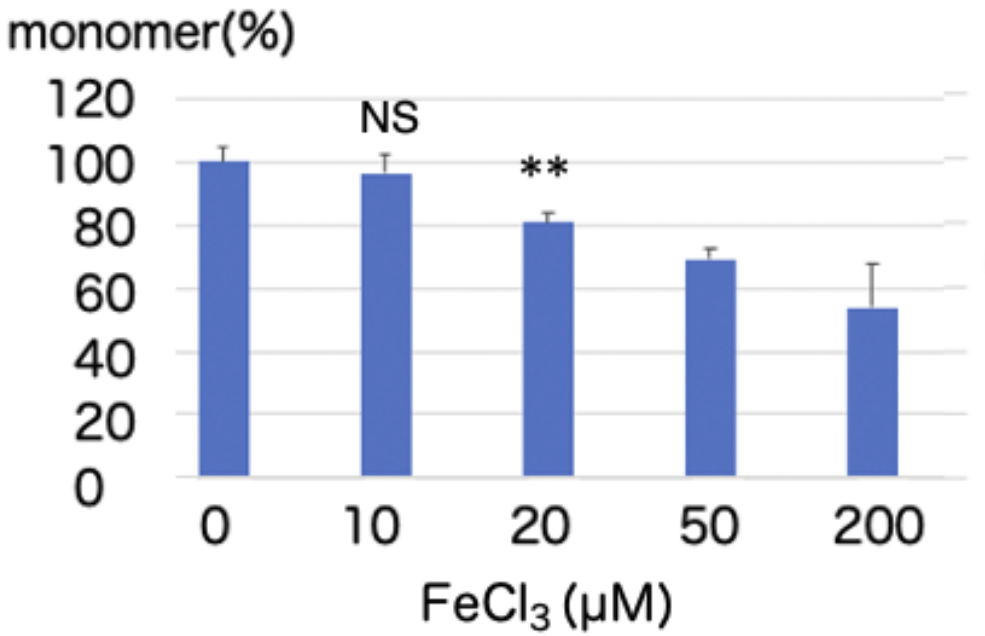
monomer(%)
120
100
80
60
40
20
0
NS
**
0
10
20
50
200
FeCl3 (μM)

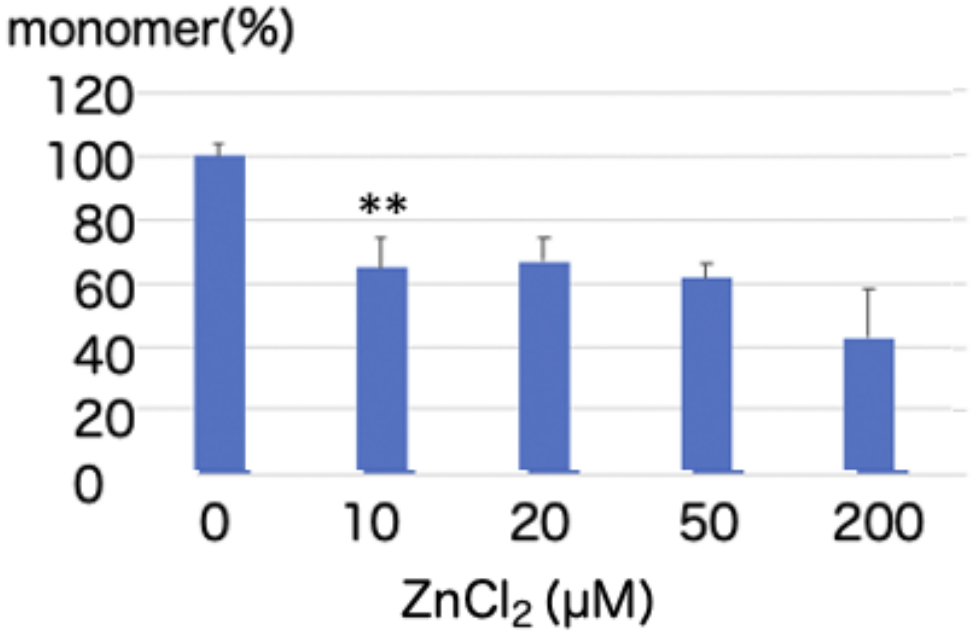
monomer(%)
120
100
80
60
40
20
0
**
0
10
20
50
200
ZnCl2 (μM)

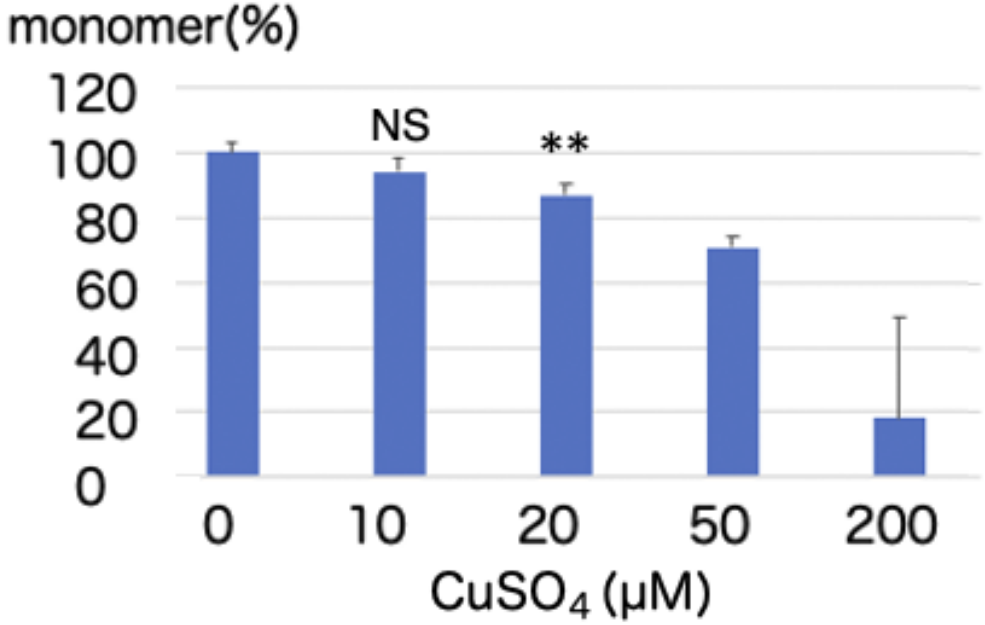
monomer(%)
120
100
80
60
40
20
0
NS
**
0
10
20
50
200
CuSO4 (μM)

w 0 1 2 0 1 2 1 2 1 2 1 2 1 2 (mM)

sup ppt sup ppt sup ppt

$FeCl_2$ $FeCl_3$ $AlCl_3$

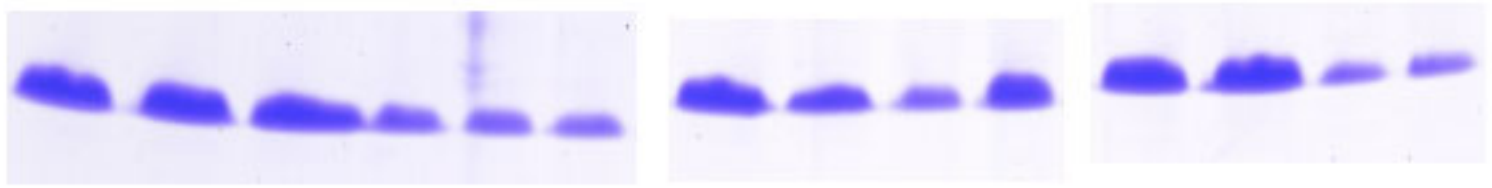

0 1 2 0 1 2 1 2 1 2 1 2 1 2 (mM)

sup ppt sup ppt sup ppt

$ZnCl_2$ $CuSO_4$ $MnCl_2$

0 1 2 0 1 2 1 2 1 2 (mM)

sup ppt sup ppt

$MgCl_2$ $CaCl_2$

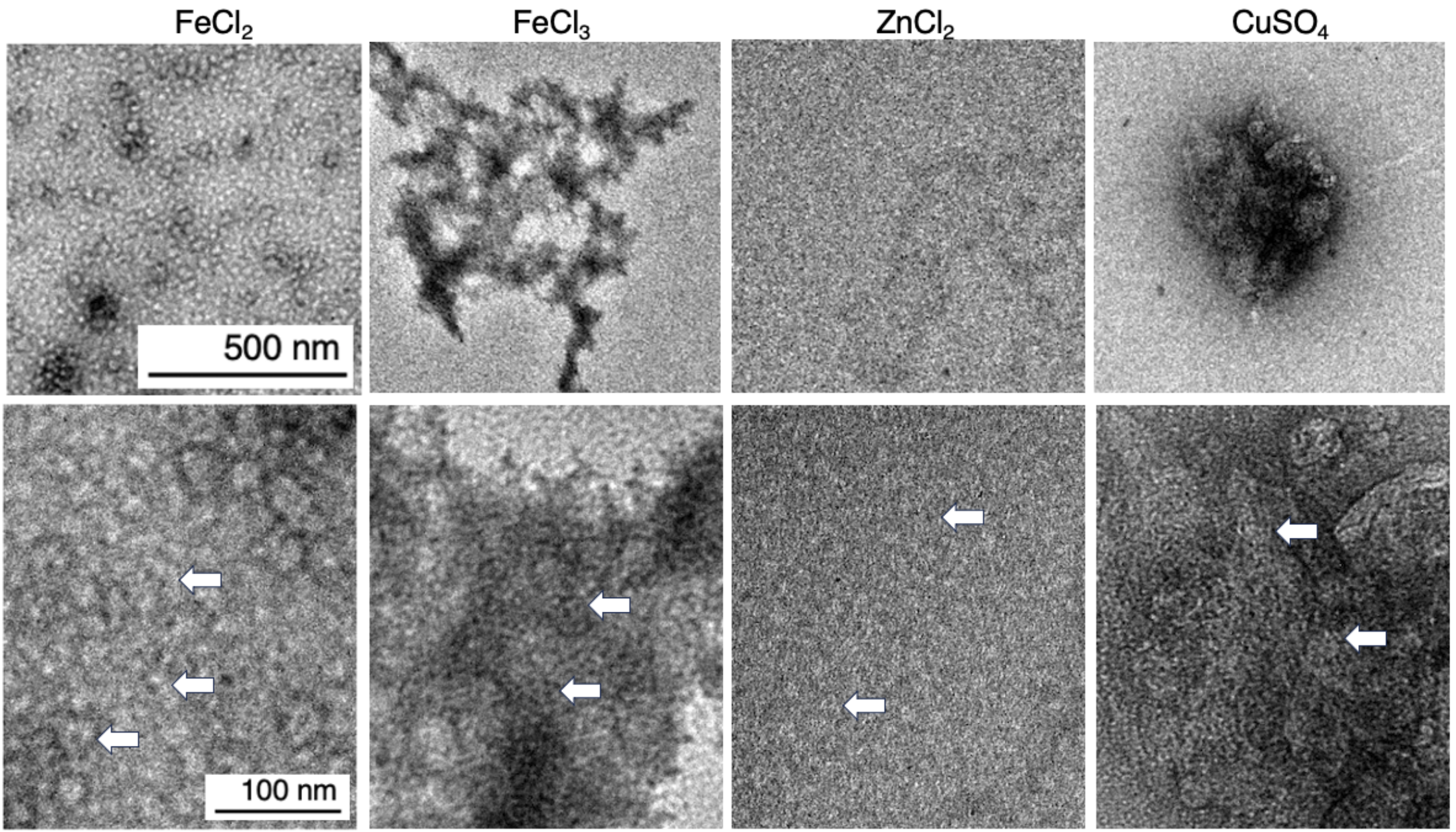
$FeCl_2$
$FeCl_3$
$ZnCl_2$
$CuSO_4$
500 nm
100 nm

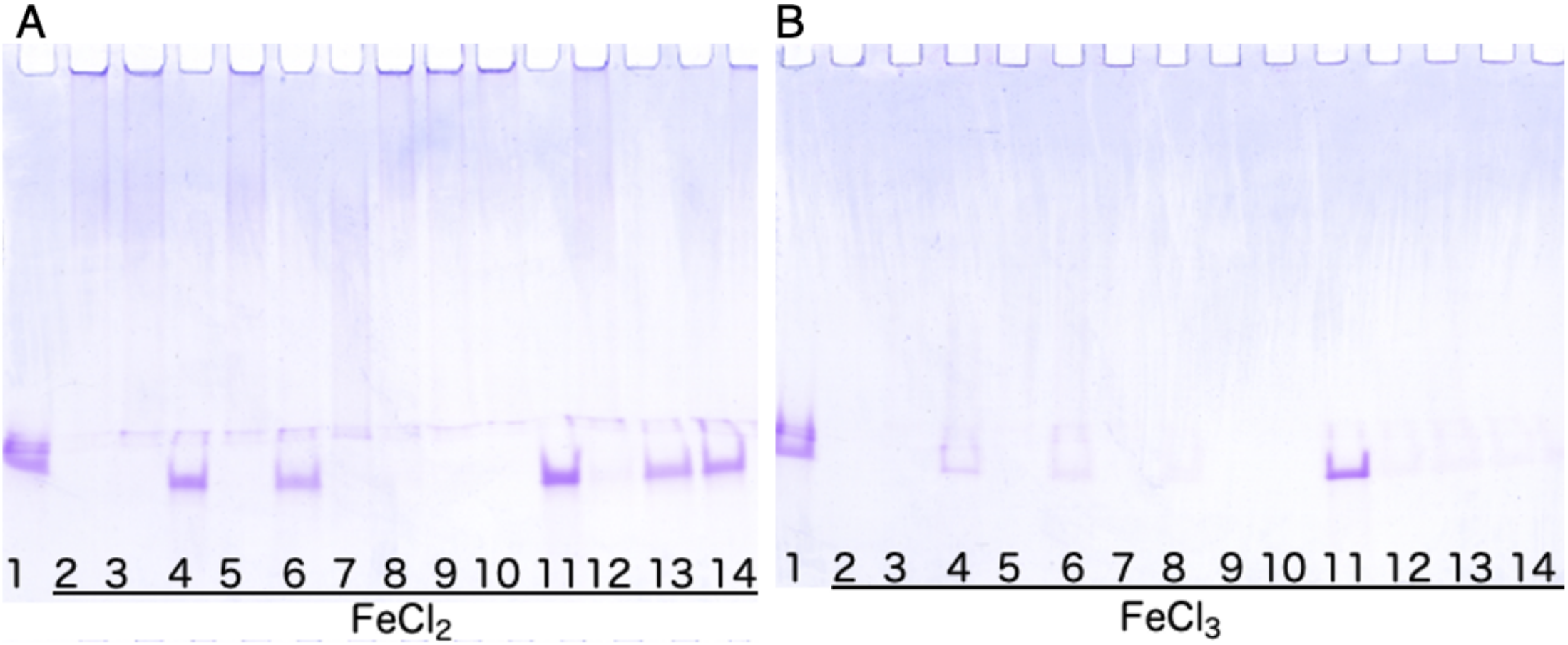

Fig. 6 Maekawa et al.